

Sub Module 2.13

Measurement of fluid velocity

Introduction:

We look at the measurement of fluid velocity in detail, in what follows. We will discuss both intrusive and non-intrusive methods, as given below:

- 1. Velocity map using Pitot tube and Pitot static tube**
 - Based on fluid mechanics principles
- 2. Hot wire anemometer**
 - Thermal effect of flow
- 3. Doppler Velocimeter**
 - Doppler effect due to scattering of waves by moving particles
- 4. Time of Flight Velocimeter**
 - Based on time of travel of sound wave through a moving medium

Items 1 and 2 are intrusive methods while item 3 is a non-intrusive method. However all these are capable of measuring local velocity of a fluid within different limits. The size of the probe tends to average the measurement over an area around the point of interest and also introduces a disturbance in the measured quantity by modifying the flow that would exist in the absence of the probe. The size of the probe should be chosen such that there are no 'blockage' effects. The term 'intrusive' refers to this aspect! The measurements also are prone to errors due to errors in alignment of the probe with respect to the flow direction. For example, a Pitot tube should be aligned with its axis facing the flow. If the flow direction is not known, it is difficult to achieve this with any great precision. One way of circumventing such a problem is to design a probe that is not very sensitive to its orientation.

1) Pitot and Pitot static tube

The basic principle of the Pitot and Pitot static tube is that the pressure of a flowing fluid will increase when it is brought to rest at a stagnation point of the probe. Figure 81 shows the streamlines in the vicinity of a blunt nosed body. We assume that, if the flow is that of a gas, like air, the velocity of the fluid is much smaller than the speed of sound in air such that density changes may be ignored. Basically the fluid behaves as an incompressible fluid. The stagnation point is located as shown. Streamlines bend past the body as shown. The pressure at the stagnation point is the stagnation pressure.

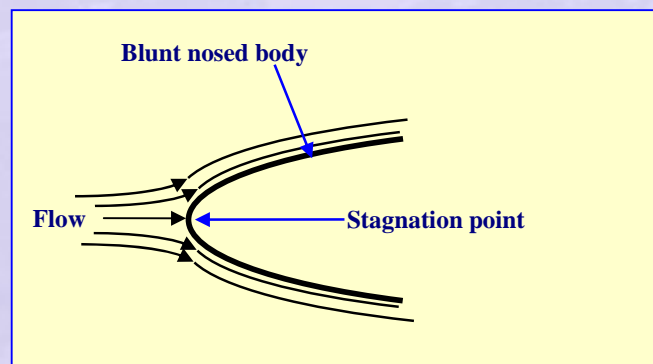


Figure 97 Flow of a fluid in the vicinity of a blunt nosed body

If viscous effects are negligible the difference between the stagnation pressure and the static pressure is related to the dynamic pressure which is related to the square of the velocity. Thus the velocity information is converted to a pressure difference that may be measured by a pressure measuring device such as a manometer.

The basic arrangement for measuring fluid velocity using a Pitot tube is shown in Figure 98. The Pitot tube consists of bent tube of small diameter (small compared to the diameter or size of the duct) with a rounded nose. The flow is axi-symmetric and in the vicinity of the nose is like the flow depicted in Figure 97. The Pitot tube is connected to one limb of a U tube manometer. The other limb of the manometer is connected to a tap made on the tube wall

as indicated. The tube tap and the nose of the Pitot tube are roughly in the same plane. It is assumed that the wall tap senses the static pressure p of the fluid while the Pitot tube senses the stagnation pressure p_o of the fluid. From Bernoulli principle we have (for low speed flow, fluid velocity much less than sonic velocity in the fluid)

$$(p_o - p) = \frac{1}{2} \rho V^2 \quad (101)$$

In Equation 101 ρ is the density (constant in the case of low speed flow) of the fluid whose velocity is being measured. We see that in case of gas flow the temperature also needs to be measured since the density is a function of static pressure and temperature. With ρ_m as the density of the manometer liquid the pressure difference is given by

$$p_o - p = (\rho_m - \rho) gh \quad (102)$$

Combining Equations 101 and 102, we get

$$V = \sqrt{2 \frac{(\rho_m - \rho)}{\rho} gh} \quad (103)$$

- Incompressible flow assumption is valid for liquid flows.
- Incompressible flow assumption is also valid for gases if the flow velocity (V) is much smaller than the speed of sound (a).
- The Mach number is defined as $M = V/a$.
- Generally density variations are important if $M \geq 0.3$ or thereabout!

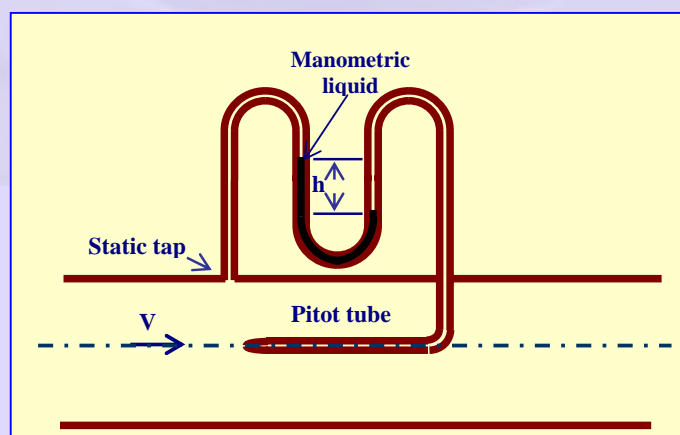


Figure 98 Pitot tube arranged to measure fluid velocity

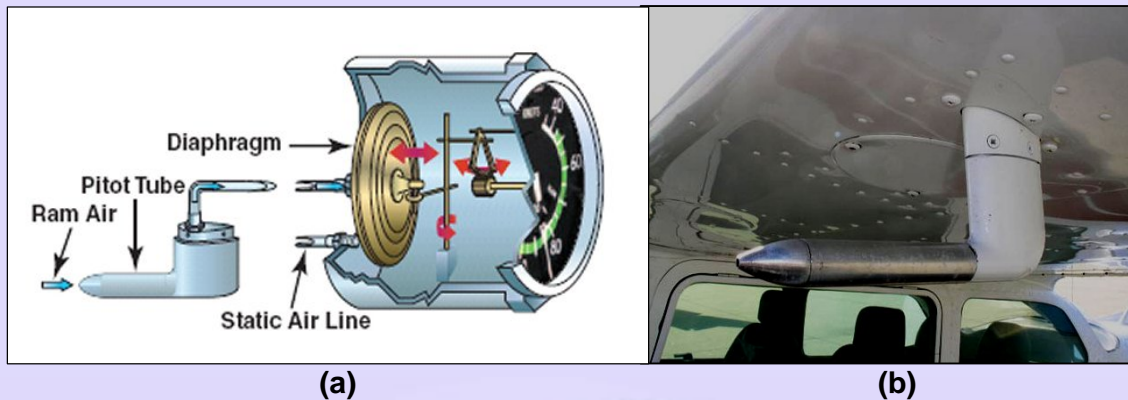


Figure 99 Measurement of speed of an aircraft using a Pitot tube

Visit <http://www.aerospaceweb.org/question/instruments/q0251.shtml>

A typical application of a Pitot tube is the measurement of velocity of an aircraft. The principle of operation of the speedometer of an aircraft is shown in Figure 99 (a). The stagnation pressure is obtained from the Pitot probe mounted on the aircraft wing as shown in Figure 99 (b). The static pressure is sensed by a static pressure hole elsewhere on the aircraft, as for example, on the fuselage. The diaphragm element (we have already seen how pressure can be converted to a displacement) with a dial indicator completes the instrument.

Many a time a Pitot static tube is made use of. Pitot static tube senses both the stagnation pressure and the static pressure in a single probe. A schematic of a Pitot static probe is shown in Figure 100. The proportions of the probe are very important in order to have accurate measurement of the velocity. Typically the probe diameter (D) would be 6 mm. The length of the probe would then be around 10 cm or more.

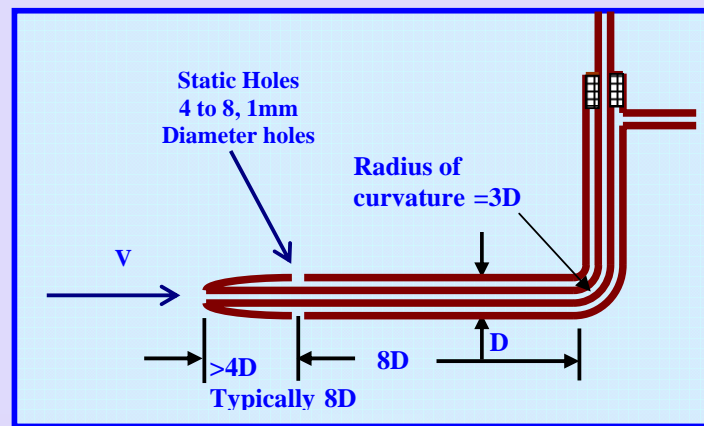


Figure 100 Pitot static tube (or Prandtl tube) showing typical proportions

The static pressure holes are positioned more than $4D$ from the stagnation point. A suitable monometer may be connected between the inner and outer tubes to measure the fluid velocity. The probe is inserted through a hole in the side of the duct or wind tunnel, as the case may be.

Example 34

- ⊙ A Pitot static tube is used to measure the velocity of an aircraft. If the air temperature and pressure are 5°C and 90 kPa respectively, what is the aircraft velocity in km/h if the differential pressure is 250 mm water column?
- ⊙ We take density of water (manometric liquid) as 999.8 kg/m^3 .
- ⊙ We calculate first the density of air at

$$p = 90 \times 10^3\text{ Pa}, T = 273 + 5 = 278\text{ K}$$

using ideal gas relation with gas constant of $R_g = 287\text{ J/kg K}$.

$$\text{⊙ We have } \rho = \frac{p}{R_g T} = \frac{90000}{287 \times 278} = 1.128\text{ kg/m}^3$$

- ⊙ The pressure difference given in terms of head of water may now be converted to SI units.

$$\Delta p = (\rho_m - \rho)gh = (999.8 - 1.128) \times 9.8 \times 0.250 = 2446.75\text{ Pa}$$

- ⊙ The aircraft speed is thus given by

$$V = \sqrt{\frac{2\Delta p}{\rho}} = \sqrt{\frac{2 \times 2446.75}{1.128}} = 65.87 \text{ m/s}$$

- ⊙ This may be specified in km/hr by noting that

$$1 \text{ km/h} = \frac{1000 \text{ m}}{3600 \text{ s}} = \frac{1}{3.6} \text{ m/s}$$

or $1 \text{ m/s} = 3.6 \text{ km/h}$

- ⊙ Thus the aircraft speed is

$$V = 65.87 \times 3.6 = 237.1 \text{ km/h}$$

- ⊙ We shall verify whether the incompressible assumption is good enough. The speed of sound is calculated by assuming that the ratio of specific heats $\gamma = 1.4$ for air. We then have the speed of sound as

$$a = \sqrt{\gamma R_g T} = \sqrt{1.4 \times 287 \times 278} = 334.2 \text{ m/s}$$

- ⊙ The corresponding Mach number is

$$M = \frac{V}{a} = \frac{65.87}{334.2} = 0.197$$

- ⊙ Since $M < 0.3$ the incompressible flow assumption may not be too bad.

Effect of compressibility

In Example 34 the Mach number of the aircraft is about 0.2. It was mentioned that the incompressible assumption may not be too bad, for this case. Let us, however, look at what will happen if the compressibility effects have to be taken into account. We discuss here subsonic flows ($M < 1$) where it may be necessary to consider the effect of density variations. In such a case we use well known relations from gas dynamics to take into account the density variations. We shall assume that the gas behaves as an ideal gas. The stagnation process (what happens near the nose of the Pitot tube) is assumed to be an isentropic process via which the flow is brought to rest from the condition upstream of the Pitot tube. From gas dynamics we have

$$\frac{p_o}{p} = \left[1 + \frac{\gamma-1}{2} M^2 \right]^{\frac{\gamma}{\gamma-1}} \quad (104)$$

Equation 102 will have to be replaced by

$$p_o - p = p \left\{ \left[1 + \frac{\gamma-1}{2} M^2 \right]^{\frac{\gamma}{\gamma-1}} - 1 \right\} = (\rho_m - \rho) gh \quad (105)$$

We may solve this for M and get

$$M = \sqrt{\frac{2}{\gamma-1} \left[\left\{ 1 + \frac{(\rho_m - \rho) gh}{p} \right\}^{\frac{\gamma-1}{\gamma}} - 1 \right]} \quad (106)$$

In fact we solve for the Mach number first and then obtain the flow velocity.

We shall look at Example 34 again using Equation 105, a little later.

In order to appreciate the above we present a plot of pressure ratio recorded by a Prandtl tube as a function of flow Mach number in Figure 101. The figure indeed shows that the incompressible assumption may be alright up to a Mach number of about 0.3. This may be appreciated better by looking at the percentage difference between the two as a function of Mach number. Such a plot is shown in Figure 102.

From Equation 104, we have $\frac{p_o}{p} = \left[1 + \frac{\gamma-1}{2} M^2 \right]^{\frac{\gamma}{\gamma-1}}$. This may be rearranged

$$\text{as } M^2 = \frac{2}{\gamma-1} \left[\left\{ \frac{p_o}{p} \right\}^{\frac{\gamma-1}{\gamma}} - 1 \right]. \text{ Let us write } \Delta p = p_o - p. \text{ Then } \frac{p_o}{p} = \frac{p + \Delta p}{p} = 1 + \frac{\Delta p}{p}.$$

Incompressible flow assumption is expected to be valid if $\Delta p \ll p$. In that case we have

$$\left(\frac{p_o}{p} \right)^{\frac{\gamma-1}{\gamma}} = \left(1 + \frac{\Delta p}{p} \right)^{\frac{\gamma-1}{\gamma}} \approx 1 + \frac{\gamma-1}{\gamma} \frac{\Delta p}{p}.$$

$$\text{Correspondingly we have } M^2 \approx \frac{2}{\gamma-1} \left[1 + \frac{\gamma-1}{\gamma} \frac{\Delta p}{p} - 1 \right] = \frac{2\Delta p}{\gamma} = \left(\frac{V}{a} \right)^2$$

With $a^2 = \frac{\gamma p}{\rho}$ we then have

$$V = \sqrt{\frac{2\Delta p}{\rho} \frac{\gamma p}{\rho}} = \sqrt{\frac{2\Delta p}{\rho}} \quad (107)$$

This is the same as expression given by Equation 103!

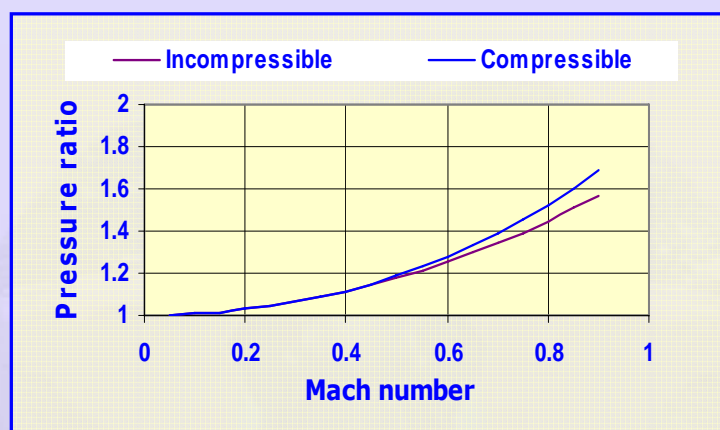


Figure 101 Pressure ratio recorded by a Prandtl tube as a function of Flow Mach number

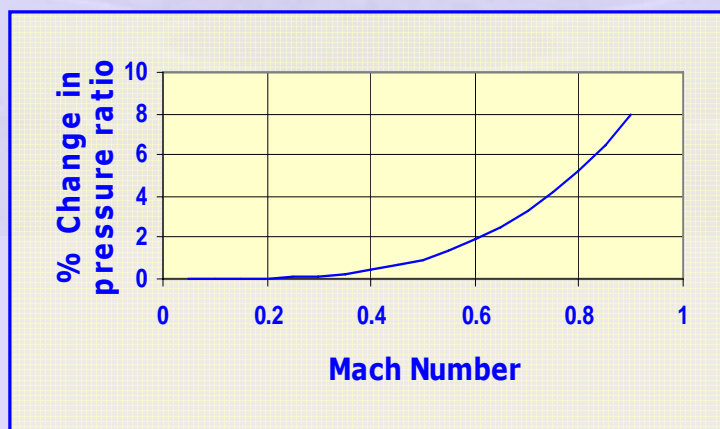


Figure 102 Percent change in Pressure ratio with compressible and incompressible assumptions recorded by a Prandtl tube as a function of flow Mach number

Example 35

- ⊙ Rework Example 34 accounting for density variations of air.

- ⊙ We take density of water (manometric liquid) as 999.8 kg/m^3 .

- ⊙ We calculate first the density of air at

$$p = 90 \times 10^3 \text{ Pa}, T = 273 + 5 = 278 \text{ K}$$

using ideal gas relation with gas constant of $R_g = 287 \text{ J/kg K}$.

- ⊙ We have $\rho = \frac{p}{R_g T} = \frac{90000}{287 \times 278} = 1.128 \text{ kg/m}^3$

- ⊙ The pressure difference given in terms of head of water may now be converted to SI units.

$$\Delta p = (\rho_m - \rho) gh = (999.8 - 1.128) \times 9.8 \times 0.250 = 2446.75 \text{ Pa}$$

- ⊙ The aircraft Mach number is given by

$$M = \sqrt{\frac{2}{\gamma - 1} \left[\left\{ 1 + \frac{\Delta p}{p} \right\}^{\frac{\gamma - 1}{\gamma}} - 1 \right]} = \sqrt{\frac{2}{(1.4 - 1)} \times \left[\left\{ 1 + \frac{2446.75}{90000} \right\}^{\frac{(1.4 - 1)}{1.4}} - 1 \right]} = 0.196$$

- ⊙ With the speed of sound of 334.2 m/s (from Example 30), the aircraft speed is given by

$$V = Ma = 0.196 \times 334.2 = 65.55 \text{ m/s} = 65.55 \times 3.6 = 235.96 \text{ km/h}$$

- ⊙ The error due to the neglect of compressibility effects is almost 1 km/h!

Example 36

- ⊙ A Pitot static tube is used to measure the velocity of water flowing in a pipe. Water of density 1000 kg/m^3 is known to have a velocity of 2.5 m/s at the position where the Pitot static tube has been introduced. The static pressure is measured independently at the tube wall and is 2 bars. What is the head developed by the Pitot static tube if the manometric fluid is mercury with density equal to 13600 kg/m^3 ?

- ⊙ From the given data, we have

$$p = 2 \text{ bars} = 2 \times 10^5 \text{ Pa}, \rho = 13600 \text{ kg/m}^3, \rho_m = 2500 \text{ kg/m}^3$$

- ⊙ Velocity of water has been specified as $V = 2.5 \text{ m/s}$

- ⊙ The dynamic pressure is given by

$$p_d = \frac{1}{2} \rho V^2 = \frac{1}{2} \times 1000 \times 2.5^2 = 3125 \text{ Pa}$$

- ⊙ This is also the pressure sensed by the Pitot static probe. Hence this must equal $(\rho_m - \rho)gh$. Thus the head developed is

$$h = \frac{p_d}{(\rho_m - \rho)g} = \frac{3125}{(13600 - 1000) \times 9.8} \text{ m} = 0.02531 \text{ m} = 25.31 \text{ mm Hg}$$

Impact probe in supersonic flow

Blunt nose impact probe:

Flow of a gas (for example air) at Mach number greater than 1 is referred to as supersonic flow. The axisymmetric flow past an impact probe (Pitot tube) in supersonic flow is very different from that in subsonic flow. Typically what happens is shown in Figure 103.

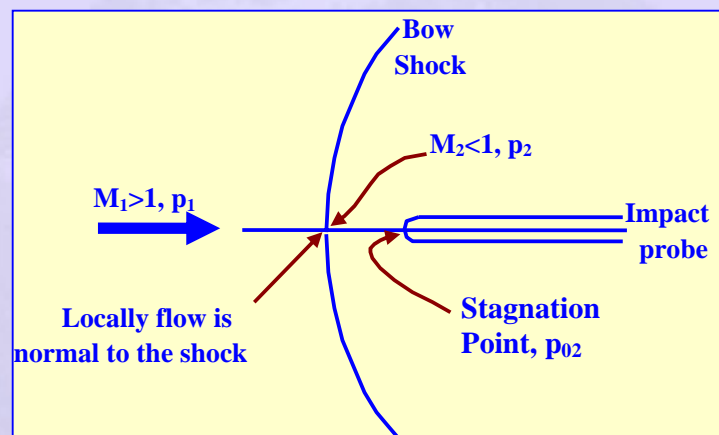


Figure 103 Supersonic flow past an impact probe

Stagnation process is more complex in the case of supersonic flow. A curved shock (referred to as a 'bow shock' because of its shape) is formed just ahead of the probe and detached from it. As is clear from the sketch the flow across the shock is normal to it just ahead of the stagnation point on the probe. The flow transforms irreversibly to subsonic flow downstream of the shock (state represented by subscript 2) from supersonic condition upstream (state represented by subscript 1) of it. The stagnation process downstream of the shock follows an isentropic process. The following expression can be derived using the appropriate relations for flow across a normal shock followed by an isentropic stagnation process (refer to a book on Gas Dynamics).

$$\frac{p_{o2}}{p_1} = \left[\frac{2\gamma M_1^2}{\gamma+1} - \frac{\gamma-1}{\gamma+1} \right] \left[1 + \frac{\gamma-1}{2} \left\{ \frac{1 + \frac{\gamma-1}{2} M_1^2}{\gamma M_1^2 - \frac{\gamma-1}{2}} \right\} \right]^{\frac{\gamma}{\gamma-1}} \quad (108)$$

Equation 108 relates the ratio of stagnation pressure measured by the impact probe to the static pressure of the flow upstream of the shock to the Mach number of the flow upstream of the shock – the quantity we are out to measure, in the first place. A plot of expression 108 is shown in Figure 104 and helps in directly reading off M_1 from the measured pressure ratio.

Wedge probe

A second type of probe that may be used for measurement of supersonic flow is the wedge type probe shown in Figure 105.

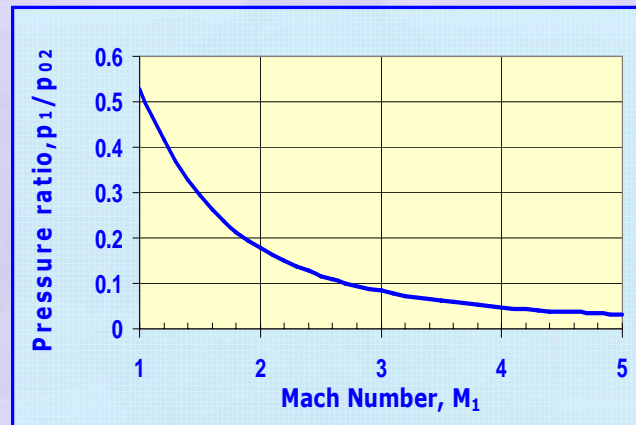


Figure 104 Pressure ratio Mach number relation for supersonic flow

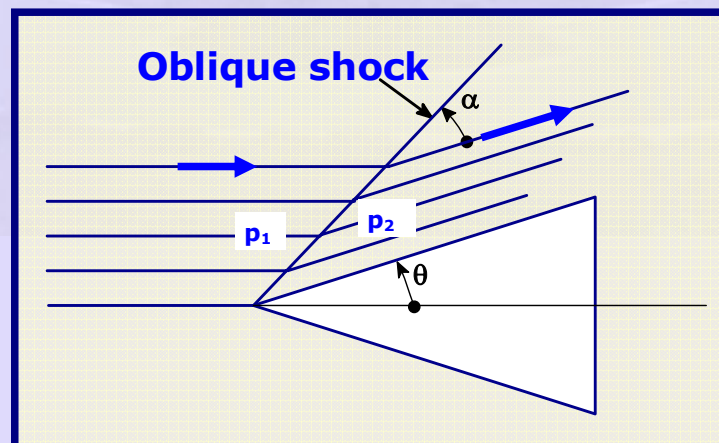


Figure 105 Wedge probe in supersonic flow

The flow past the wedge is two dimensional with an oblique shock emanating from the apex of the wedge as shown. The flow becomes parallel to the

wedge surface downstream of the oblique shock. The static pressure p_2 may be sensed by using a static pressure tap on the surface of the wedge some distance away from the apex. The relationship between the pressures upstream and downstream of the oblique shock is given by

$$\frac{p_2}{p_1} = \frac{2\gamma}{\gamma+1} M_1^2 \sin^2 \alpha - \frac{\gamma-1}{\gamma+1} \quad (109)$$

The shock angle α itself is a function of M_1 and θ . Tables relating these are available in books on Gas Dynamics. One may also use the web resource at <http://www.aero.ltr.tudelft.nl/~bert/shocks.html> to calculate these.

Example 37

⊙ A wedge probe has a wedge angle of $\theta = 8^\circ$ and placed in a wind tunnel where the flow is known to be at $M_1 = 1.5$. Calculate the static pressure ratio that is expected from the probe.

⊙ We use the web resource and input $M_1 = 1.5$ and turn angle (weak shock) as $\theta = 8^\circ$. The oblique shock calculator yields the following:

(The entries have been edited to show only three digits after the decimal point and angle with two digits after the decimal point)

⊙ Oblique Shock Relations Perfect Gas, Gamma =

Angles in degrees.

INPUT: $M_1 =$ Turn angle (weak shock)

$M_2 =$	<input type="text" value="1.208"/>	$\theta =$	<input type="text" value="8"/>	$\alpha =$	<input type="text" value="52.57"/>
$p_2/p_1 =$	<input type="text" value="1.489"/>	$\rho_2/\rho_1 =$	<input type="text" value="1.326"/>	$T_2/T_1 =$	<input type="text" value="1.122"/>
$p_{02}/p_{01} =$	<input type="text" value="0.994"/>	$M_{1n} =$	<input type="text" value="1.191"/>	$M_{2n} =$	<input type="text" value="0.848"/>

⊙ Thus we see that the oblique shock makes an angle of 52.57° .

Substitute this in to Equation 109 to get

$$\frac{p_2}{p_1} = \frac{2 \times 1.4}{1.4 + 1} (1.5 \times \sin 52.57^\circ)^2 - \frac{1.4 - 1}{1.4 + 1} = 1.489$$

⊙ This will correspond to the pressure ratio indicated by the probe.

More impact probes:

It should be clear by now that a probe in supersonic flow is a device that produces a change in the pressure that may be measured. The wedge probe is an example of this. Another example is a probe having cone-cylinder configuration as shown in Figure 106.

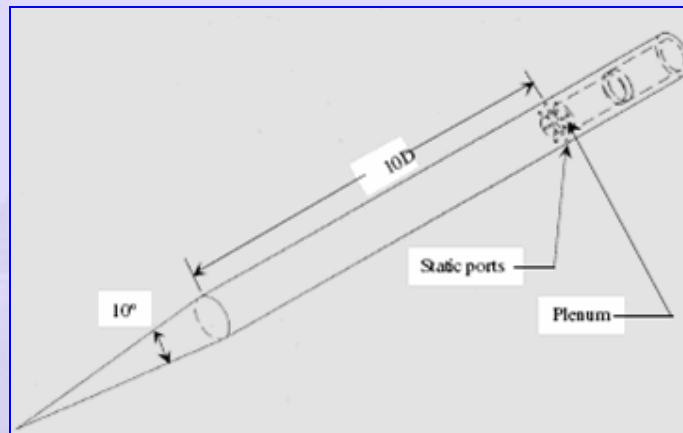


Figure 106 Cone-cylinder probe for supersonic flow

A.R. Porro, Pressure Probe Designs for Dynamic Pressure Measurements in Supersonic Flow Field, NASA/TM-2001-211096

The probe diameter used was 0.4435 inch or 11.05 mm. Three different probe tips were used, the one shown in the figure being for the measurement of static pressure. Eight static pressure ports are positioned 10 D from the cone shoulder. This design gives accurate flow field static pressure according to the author.

Orientation effects:

The sensitivity to orientation is also a concern while using probes in subsonic as well as supersonic flows. It is also possible that the flow direction may be determined, when it not known, by using this sensitivity. A multiple hole probe (multi-hole probe, for short) is used for this purpose. Examples of miniature multi-hole probes for subsonic flow applications are shown in Figure 107 (size is inferred by the built in scale).

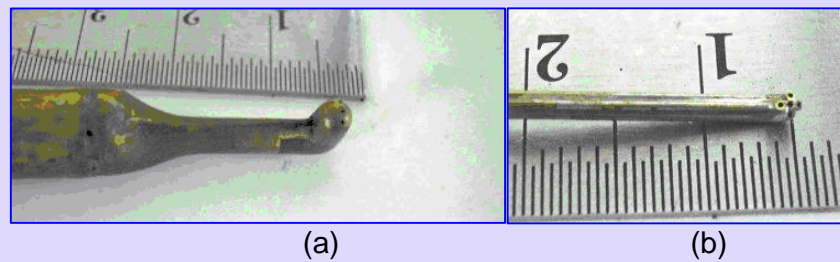


Figure 107 Miniature (a) three hole and (b) five hole probes for subsonic flow

Visit: <http://www.ltt.ntua.gr/probes.html>

These pictures have been sourced from the Laboratory of Turbo-machines,
National University of Athens

We shall explain the basic principle involved in multi-hole probes. Take, for example, a three hole probe oriented such that the plane passing through the three holes also contains the plane in which the two dimensional flow is taking place. The state of affairs, in general, is as shown in Figure 108.

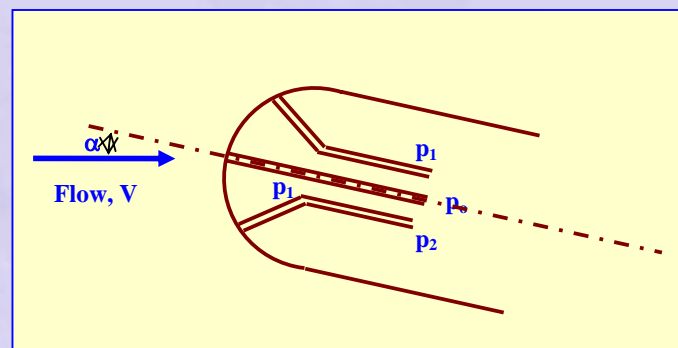


Figure 108 Schematic of three hole probe oriented at an angle to the oncoming flow

We know from fluid flow theory that the pressure is a function of angle the static hole makes with respect to the direction of flow. Since the axis of the probe is pitched at an angle α as shown, the effective angle made by hole p_1 is greater than the angle made by hole p_2 . The pressure difference $(p_o - p_1)$ is different from the pressure difference $(p_o - p_2)$. When the probe is aligned with zero pitch the two are equal and thus helps to identify the flow direction. Also the pressure difference $(p_1 - p_2)$ is zero when the pitch angle is zero or when the probe is facing the flow normally.

The argument may be extended to a five hole probe. There are two pressure differences, $(p_1 - p_4)$ and $(p_2 - p_3)$ that may be monitored. These differences will be functions of two angles, pitch angle α (as in the case of the three hole probe) and the roll angle β as shown in Figure 109.

Calibration of three and five hole probes is done by changing the roll and pitch angles systematically in a wind tunnel where the direction of flow is known, collecting the pressure difference data and evolving a relationship between these and the two angles. It is usual to represent the data in terms of pressure coefficients defined by

$$C_p = \frac{\Delta p}{\frac{1}{2} \rho V^2} \quad (110)$$

It is seen that the pressure coefficient C_p is non-dimensional and the dynamic pressure is used as the reference. Each and every multi-hole probe needs to be calibrated because of small variations that are always there between different probes during the manufacturing process. More details about multi-hole probes and their calibration may be obtained from specialized literature.

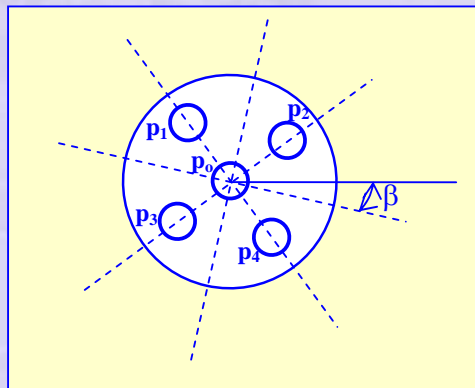


Figure 109 Schematic of a five hole probe showing the roll angle

2) Hot wire anemometer

A hot wire anemometer basically involves the power that is dissipated by a hot wire to an ambient fluid that is moving past it. The larger the velocity of the fluid, larger the heat dissipation from the wire – for a fixed wire temperature. Alternately - larger the velocity of the fluid, smaller the wire temperature – for a fixed heat dissipation rate from the wire. Thus a hot wire anemometer is a thermal device and the velocity information is converted to thermal – either temperature change or change in the heat dissipation rate – information.

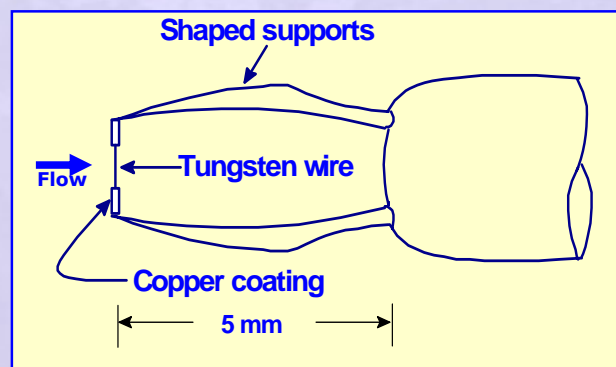


Figure 110 Typical hot wire probe

Typical hot wire probe element is shown in Figure 110. It consists of a very small diameter (a few μm) and a couple of mm long tungsten wire tightly fixed between supports that also act as electrical connections to external electrical circuit. The wire is heated by passing a current I through it. Let the resistance of the tungsten wire be R_w . We assume that the wire resistance is a linear function of temperature and is given by

$$R_w = R_\infty [1 + b(T_w - T_\infty)] \quad (111)$$

In the above the subscript ∞ refers to a reference state, b is temperature coefficient of resistance and R_∞ is the wire resistance at the reference temperature. The temperature coefficient is $3.5 \times 10^{-3}/^\circ\text{C}$ for Platinum while it is $5.235 \times 10^{-3}/^\circ\text{C}$ for tungsten. The heat dissipated by the wire is given by

$I^2 R_w$ and must equal the heat loss from the wire surface given by $\pi DLh(T_w - T_\infty)$, under steady state. Thus

$$I^2 R_w = \pi DLh(T_w - T_\infty) \quad (112)$$

In the above expression D is the diameter of the wire, L is the effective length of the wire and h is the heat transfer coefficient. The heat transfer coefficient h (we assume that the hot wire element is like a cylinder in cross flow) follows the so called King's law which state that

$$\pi DLh = A + BV^n \quad (113)$$

Here A, B and index n are constants, usually determined by calibration and V is the fluid velocity. The constant part of the heat transfer coefficient accounts for natural convection and radiation even when the fluid is stationary. The variable part accounts for forced convection heat transfer in the presence of a moving fluid. The power law dependence is the observation of King. We have seen earlier while discussing heat transfer to a thermometer well that the power law form appears in the Zhukaskas correlation for flow normal to a cylinder. From Equation 111 we have

$$T_w - T_\infty = \frac{R_w - R_\infty}{bR_\infty} \quad (114)$$

Substituting these in Equation 112, we get $I^2 R_w = (A + BV^n) \frac{(R_w - R_\infty)}{bR_\infty}$ which may be rearranged to read

$$A + BV^n = \frac{I^2 R_w R_\infty b}{(R_w - R_\infty)} \quad (115)$$

Equation 115 is the basic hot wire anemometer equation. There are two ways of using the hot wire probe.

- a) Constant Temperature or CT anemometer: The hot wire is operated at constant temperature and constant R_w . The current I will respond to changes in the velocity V.

- b) Constant Current or CC anemometer The hot wire current is held fixed.
The resistance of the wire responds to change in the velocity V.

a) Constant Temperature or CT anemometer:

A bridge circuit (Figure 111) is used for the constant temperature operation of a hot wire anemometer. The series resistance R_s is adjusted such that the bridge is at balance at all times. Thus, if the fluid velocity increases more heat will be dissipated by the hot wire at a given temperature and hence the current needs to increase. This is brought about by decreasing R_s . The opposite is the case when the fluid velocity decreases. We may write the power dissipated by the hot wire element as $I^2 R_w = \frac{E^2}{R_w}$. Here E is the voltage across the hot wire that is measured by the voltmeter as shown in Figure 111.

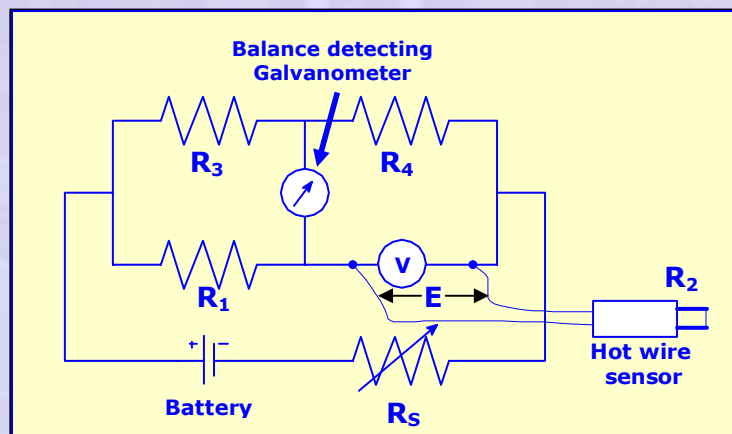


Figure 111 Hot wire bridge circuit for constant temperature operation

Equation 115 then takes the form

$$A + BV^n = \frac{E^2}{R_w} \frac{R_\infty b}{(R_w - R_\infty)} \quad (116)$$

We note that, under CT operation, except E all other quantities on the right hand side are constant. We may absorb these in to the constants A and B to write the above equation in the form

$$E^2 = A + BV^n \quad (117)$$

Let E_o be the output of the sensor when $V = 0$. The constant A is then nothing but E_o^2 . Hence we have

$$E^2 - E_o^2 = BV^n \text{ or } \left(\frac{E}{E_o} \right)^2 - 1 = \left(\frac{B}{E_o^2} \right) V^n \quad (118)$$

If we take logarithms on both sides, the following equation results:

$$\log \left[\left(\frac{E}{E_o} \right)^2 - 1 \right] = \log \left(\frac{B}{E_o^2} \right) + n \log V \quad (119)$$

The above expression is a linear representation of the output, obtained by suitable mathematical manipulations. Example 38 demonstrates these aspects.

Useful heat transfer correlation

The correlation due to Churchill and Bernstein is useful as long as the Peclet number (product of Reynolds and Prandtl numbers) is greater than 0.2. We shall assume a constant Prandtl number for air as 0.7. The above condition means that the Reynolds number should be greater than about 0.3 for the correlation to hold. We note that the wire diameter in a hot wire sensor is such that this condition is quite a limitation in the use of the correlation. The correlation itself is given by

$$Nu = 0.3 + \frac{0.62 Pr^{\frac{1}{3}}}{\left[1 + \left(\frac{0.4}{Pr} \right)^{\frac{2}{3}} \right]^{\frac{4}{3}}} \sqrt{Re} \quad (120)$$

With $Pr = 0.7$, this takes the form

$$Nu = 0.3 + 0.362 \sqrt{Re} \quad (121)$$

Note that Nu is the Nusselt number based on wire diameter as the characteristic dimension. In fact, King proposed a relation of the above form

based on empirical observations. The properties such as kinematic viscosity and thermal conductivity of air are at the mean film temperature.



Example 38

- ⊙ A hot wire operates at a temperature of 200°C while the air temperature is 20°C. The velocity of air may vary between 0 and 10 m/s. The hot wire element is a platinum wire of 4 μm diameter and 1.2 mm length. What is the sensor output when the air velocity is 4 m/s?

- ⊙ Diameter and length of the hot wire element are:

$$D = 4 \mu m = 4 \times 10^{-6} m, L = 1.2 mm = 0.0012 m$$

- ⊙ We take electrical resistivity of Platinum at 20°C as $\rho_{20} = 10.5 \times 10^{-8} \Omega m$.

We also assume a value of $b = 0.00385 / ^\circ C$ as the temperature coefficient of Platinum. Further, we assume that the resistivity of Platinum varies linearly according to the relation $\rho_t = \rho_{20} [1 + b(t - 20)]$ where t is the temperature in °C. Since the sensor operates in the CT mode, the wire resistance is constant and is given by

$$\begin{aligned} R_w &= R_{20} [1 + b(t - 20)] = \frac{\rho_{20} L}{\frac{\pi}{4} D^2} [1 + b(t - 20)] \\ &= \frac{10.5 \times 10^{-8} \times 0.0012}{\frac{\pi}{4} \times (4 \times 10^{-6})^2} [1 + 0.00385(200 - 20)] = 17.1 \Omega \end{aligned}$$

- ⊙ The heat transfer coefficient is estimated using the correlation due to Churchill and Bernstein. The properties of air are taken at the film

temperature of $T_m = \frac{t + t_\infty}{2} = \frac{200 + 20}{2} = 110^\circ C$. The required properties

from air tables are $\nu_m = 24.15 \times 10^{-6} m^2 / s$, $k_m = 0.032 W / m^\circ C$

- ⊙ The Reynolds number is calculated as

$$Re = \frac{VD}{\nu_m} = \frac{4 \times 4 \times 10^{-6}}{24.15 \times 10^{-6}} = 0.663$$

- ⊙ With Pr = 0.7, the Nusselt number is calculated as

$$Nu = 0.3 + 0.362 \times \sqrt{0.663} = 0.595$$

- ⊙ The heat transfer coefficient is then given by

$$h = \frac{Nu k_m}{D} = \frac{0.595 \times 0.032}{4 \times 10^{-6}} = 4758 \text{ W / m}^2\text{°C}$$

- ⊙ Heat dissipation from the wire when exposed to an stream at 4 m/s is then given by

$$Q = \pi D L h (t - t_\infty) = \pi \times 4 \times 10^{-6} \times 0.0012 \times 4758 \times (200 - 20) = 0.0129 \text{ W}$$

- ⊙ This must equal $\frac{E^2}{R_w}$ and hence the output of the sensor is

$$E = \sqrt{Q R_w} = \sqrt{0.0129 \times 17.1} = 0.470 \text{ V}$$

We make a plot of sensor output as a function of the air velocity using the range from 0 to 10 m/s for it. The plot (Figure 112) indicates that the response is indeed non-linear. However we linearise the output as indicated earlier by making a log-log plot as shown in Figure 113. On both plots we have shown the response at air velocity of 4 m/s corresponding to the case considered in Example 38.

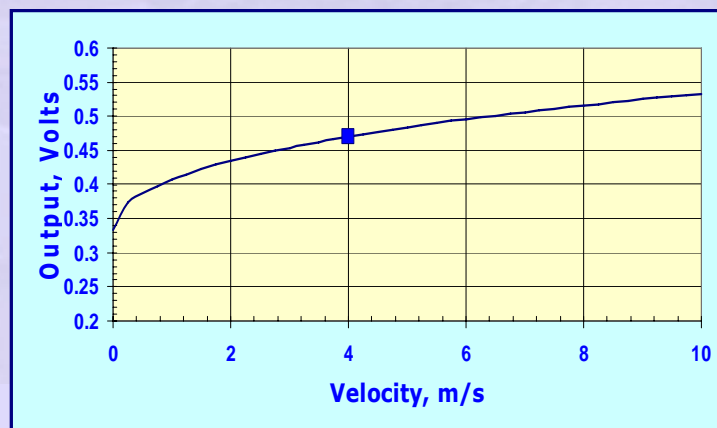


Figure 112 Response of hot wire sensor of Example 35 in CT mode

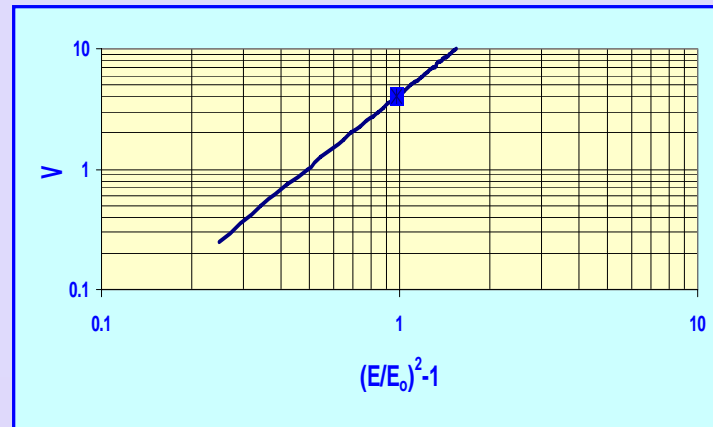


Figure 113 Linearised output of hot wire sensor of Example 35 in CT mode

b) Constant Current or CC anemometer

In this mode of operation the current through the sensor wire is kept constant by an arrangement schematically shown in Figure 114. As the sensor resistance changes the series resistance is adjusted such that the total resistance and hence the current remains fixed. The potential drop across the sensor thus changes in response to a change in its resistance. This voltage is amplified, if necessary, before being recorded.

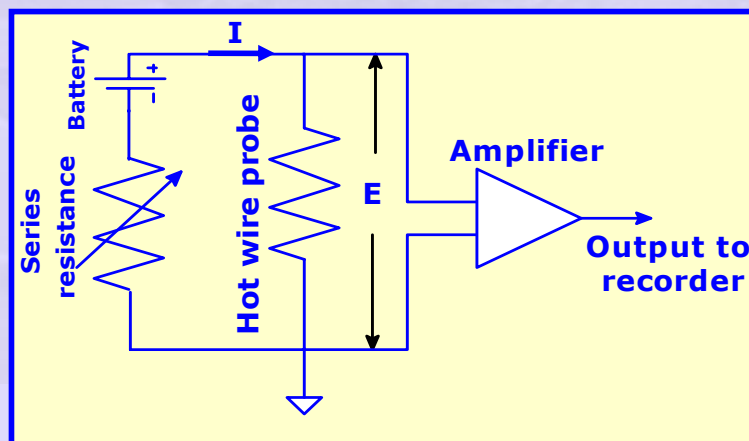


Figure 114 Hot wire circuit for constant current operation

Referring to Figure 114 we see that the output of the circuit E is proportional to IR_w . Since I is constant in CC mode of operation, R_w may be replaced by E , the voltage in the presence of fluid flowing at velocity V normal to the hot wire. Similarly we may replace R_∞ by E_∞ . We also represent the output of the

sensor when the velocity of the fluid is zero as E_o . With these, Equation 115 takes the form

$$A + BV^n = \frac{bEE_\infty}{I(E - E_\infty)} \quad (122)$$

We also have

$$A = \frac{bE_oE_\infty}{I(E_o - E_\infty)} \quad (123)$$

Equation 123 helps in getting E_∞ as $E_\infty = \frac{AE_o}{A + \frac{b}{I}E_o}$. Introduce this in Equation

122 to get

$$A + BV^n = \frac{b}{I} \frac{E \left(\frac{AE_o}{A + \frac{b}{I}E_o} \right)}{\left(E - \frac{AE_o}{A + \frac{b}{I}E_o} \right)} = \frac{b}{I} \frac{AEE_o}{\left(E \left\{ A + \frac{b}{I}E_o \right\} - AE_o \right)}. \quad \text{The denominator on the}$$

right hand side may be rewritten

as $E \left\{ A + \frac{b}{I}E_o \right\} - AE_o = (E - E_o) \left\{ A + \frac{b}{I}E_o \right\} + \frac{b}{I}E_o^2$. Then the above equation

may be rearranged as

$$(E - E_o) \underbrace{\left\{ A + \frac{b}{I}E_o \right\}}_{K_1} + \underbrace{\frac{b}{I}E_o^2}_{K_2} = \underbrace{\frac{AE_o b}{I}}_{K_3} (E - E_o) \frac{1}{A + BV^n} + \underbrace{\frac{AE_o^2 b}{I}}_{K_4} \frac{1}{A + BV^n}$$

This may further be rearranged as

$$(E - E_o) \left(K_1 - \frac{K_3}{A + BV^n} \right) = \frac{K_4}{A + BV^n} - K_2$$

Finally we get

$$(E_o - E) = \frac{\overbrace{K_2 BV^n}^{A_1} - \overbrace{(K_4 - K_2 A)}^{=0}}{\underbrace{(K_1 A - K_3)}_{=A^2=A_2} + \underbrace{K_1 BV^n}_{A_3}} = \frac{A_1 V^n}{A_2 + A_3 V^n} = \frac{a_1 V^n}{1 + a_2 V^n} \quad (124)$$

In the above expression $a_1 = \frac{A_1}{A_2}$ and $a_2 = \frac{A_3}{A_2}$. The output response thus involves two constants that may be determined by suitable calibration.

Response of a hot wire anemometer operating in the CC mode is typically like that shown in Figure 115.

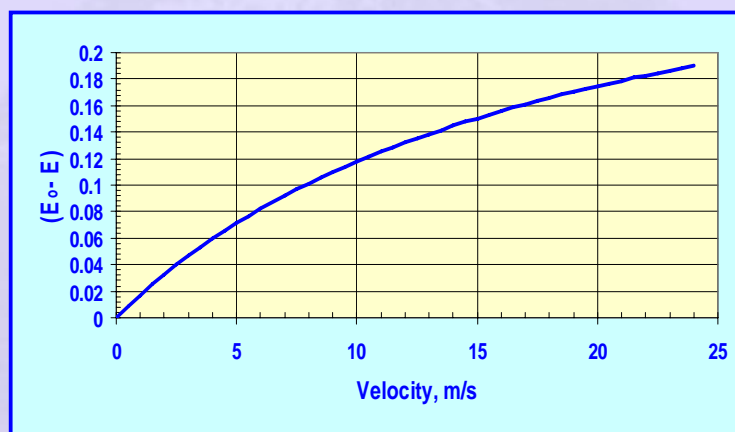


Figure 115 Output of a typical micro machined hot wire probe in the CC mode

Length of wire = 100 μm , Resistance at room temperature = 2000 Ω

Practical aspects:

Hot wire probes are very delicate and need to be handled very carefully. Rugged probes are made using a film of Platinum deposited on a substrate rather than using a wire. Two such designs are shown in Figures 116 and 117 below.

The probe shown in Figure 116 is cylindrical while the probe shown in Figure 117 is in the shape of a wedge. A thin film of Platinum is used as the sensor. It is usually protected by a layer of alumina or quartz. The substrate provides ruggedness to the film while the protective coating provides abrasive resistance. The active length of the sensor is between the gold plated portions. The leads are gold wires (Figure 116) or gold film (Figure 117). In

the case of wire type probes it is advisable not to expose the wire to gusts of fluid. The sensor must be handled gently without subjecting it to excessive vibration.

A typical hot wire system that is supplied by “**topac**” has specifications given in Table 18.

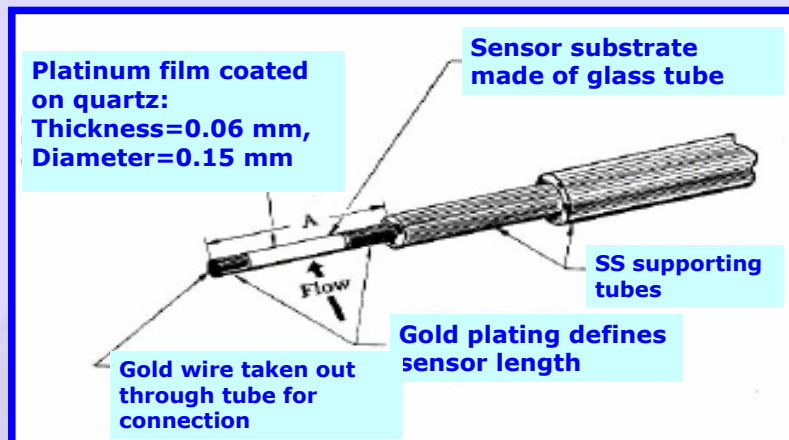


Figure 116 Hot film transducer in the form of a cylinder

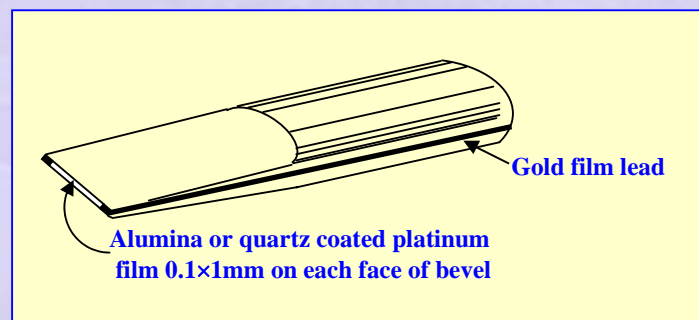


Figure 117 Hot film wedge probe

Measurement of transients (velocity fluctuations)

Hot wire anemometer is routinely used for the measurement of velocity fluctuations that occur, for example, in turbulent flows. The time constant of the sensor plays an important role in determining the frequency response of the hot wire. Take for example the hot wire that was considered in Example 38. Suppose the mean velocity at a certain location in the flow is 4 m/s. The fluctuating component will be superposed on this mean velocity. Let us

assume that the fluctuation is small compared to the mean. The time constant may then be based on the conditions that prevail at the mean speed.

The heat transfer coefficient was obtained as $h = 4758 \text{ W/m}^2\text{°C}$. Thermal conductivity of Platinum is $k = 69 \text{ W/m°C}$. With the diameter $D = 4 \text{ }\mu\text{m}$ as the characteristic dimension, the Biot number is

$$Bi = \frac{hD}{k} = \frac{4758 \times 4 \times 10^{-6}}{69} = 0.00028. \text{ The hot wire element may be treated as}$$

lumped system of first order. The time constant may now be estimated. The density and specific heat of Platinum are taken as $\rho = 21380 \text{ kg/m}^3$ and $c = 134 \text{ J/kg°C}$. The volume to surface area ratio for the wire is

$$\frac{V}{S} = \left(\frac{\pi D^2}{4} L \right) \div (\pi DL) = \frac{D}{4} = 10^{-6} \text{ m}. \text{ The first order time constant is then}$$

obtained as

$$\tau = \left(\frac{\rho c}{h} \right) \left(\frac{V}{S} \right) = \left(\frac{21380 \times 134}{4758} \right) \times 10^{-6} = 0.0006 \text{ s} \quad (125)$$

The corresponding bandwidth may be calculated as

$$f = \frac{1}{2\pi\tau} = \frac{1}{2 \times \pi \times 0.0006} = 265 \text{ Hz} \quad (126)$$

This may not be good enough for measurements of transients that occur in turbulent flows. Literature reports hot wire probes with time constant as low as $2 \text{ }\mu\text{s}$ (F. Jiang, Y. C. Tai, C. H. Ho, and W. J. Li. A Micromachined Polysilicon Hot-Wire Anemometer. *Solid-State Sensor and Actuator Workshop, Hilton Head, SC*, pp. 264-267, 1994). Hot wire anemometer system AN-1003 supplied by A A Lab Systems USA has a frequency response in excess of around 10 kHz (Visit <http://www.lab-systems.com/products/flow-mea/an1003/techspec.htm>).

Table 18 Specifications of a typical hot wire anemometer

AF210 series Specifications: Hot Wire Anemometer	
Range Flow 0.1 m/s 10.00 m/s	Accuracy $\pm 0.12 \text{ m/s} \pm 1\% \text{ reading}$ ($+5^\circ$ to $+45^\circ\text{C}$) $\pm 0.20 \text{ m/s} \pm 2\% \text{ reading}$ -20°C to $+5^\circ\text{C}$ & $+45^\circ\text{C}$ to $+70^\circ\text{C}$
Operating temperature	0 to $+50^\circ\text{C}$
Operating temperature probe tip	-20 to $+80^\circ\text{C}$
Probe length	300 mm plus handle
Probe Diameter	13 mm
Dimensions	140 x 79 x 46 mm
Weight	250 gm

From www.topac.com



3) Doppler Velocimeter

As mentioned earlier this is basically a non intrusive method of velocity measurement. This method of velocity measurement requires the presence of scattering particles in the flow. Most of the time these are naturally present or they may be introduced by some means. The Doppler effect is the basis for the measurement. Doppler effect may be used with waves of different types –electromagnetic waves: visible, IR, micro wave, ultrasound. We explain the Doppler effect by referring to Figure 118.

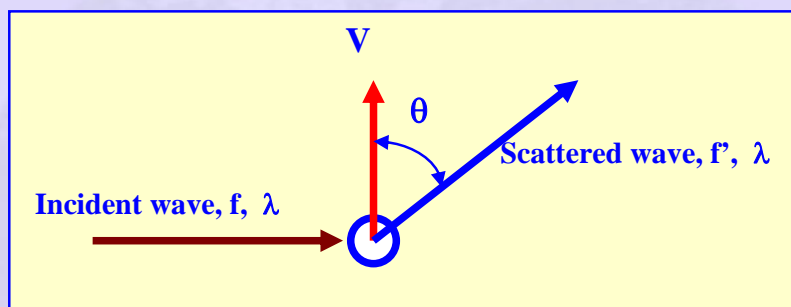


Figure 118 Scattering of radiation by a moving particle

Let the particle move with a velocity V in a medium in which the wave propagates at speed c . The incident wave is characterized by wavelength λ and frequency f and is incident along a direction that is normal to the velocity V of the scattering particle. We make observation of the wave scattered along a direction that makes an angle θ with respect to the direction of V , as shown. Incident wave wavelength and frequency are related through the well know relation

$$f = \frac{c}{\lambda} \quad (127)$$

It has been observed that the frequency of the scattered wave is different from the frequency of the incident wave because of the motion of the scattering particle. The incident wave travels at the wave speed c while the scattered wave travels at an enhanced speed due to the component of the particle velocity that is added to it. The wavelength does not change. The frequency

of the wave alone undergoes a change. Hence, we have, for the scattered wave

$$f' = \frac{c + V \cos \theta}{\lambda} \quad (128)$$

The difference between the two frequencies is referred to as the Doppler shift. It is given by

$$f_D = f' - f = \frac{c + V \cos \theta}{\lambda} - \frac{c}{\lambda} = \frac{V \cos \theta}{\lambda} \quad (129)$$

The general case where the wave is incident along a direction that makes an angle θ_i and is scattered along a direction that makes an angle θ_s with the direction of the particle velocity is shown in Figure 119. Note that the incident and scattered waves need not be in the same plane even though Figures 118 and 119 have been drawn on this basis.

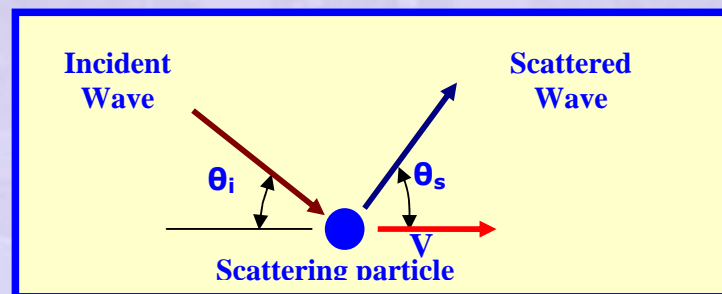


Figure 119 General case of scattering of an incident wave by a moving particle

The Doppler shift in this case is easily seen to be

$$f_D = \frac{V}{\lambda} (\cos \theta_s - \cos \theta_i) \quad (130)$$

It is clear from these expressions that the Doppler shift will occur only if the particle has non-zero component along the direction of travel of the wave.

We take an example of light wave of $\lambda = 0.68 \mu\text{m}$. The speed of light in air may be taken as $c = 3 \times 10^8 \text{ m/s}$. The light wave being considered is actually laser light from a Helium-Neon laser. The frequency of the light wave is $f = \frac{c}{\lambda} = \frac{3 \times 10^8}{0.68 \times 10^{-6}} = 4.412 \times 10^{14} \text{ Hz}$. Consider the scattering of this wave by a particle traveling with a velocity of 10 m/s as shown in Figure 101. The Doppler shift is given by $f_D = \frac{V \cos \theta}{\lambda} = \frac{10 \cos \theta}{0.68 \times 10^{-6}} = 14.706 \cos \theta \text{ MHz}$. The Doppler shift follows a cosine distribution. Doppler shift of $\pm 14.7 \text{ MHz}$ occurs respectively for $\theta = 0$ (forward scatter) and $\theta = \pi$ (backward scatter). The Doppler shift is zero when $\theta = \pm \pi/2$.

Ultrasonic Doppler velocity meter

The first device we shall consider is one that uses ultrasound (sound waves above 20 kHz and typically 100 kHz) as the beam that undergoes Doppler shift due to a moving particle. These are in very common use in medicine, specifically for blood flow measurements in patients. The ultrasound waves are produced by a piezoelectric crystal driven by an ac source at the desired frequency. This transducer may be used as a transmitter as well as a receiver. The construction details of a transducer are shown in Figure 120. The transducer consists of a small cylindrical piece of a piezoelectric crystal that is mounted in a casing with a backing of absorbing material. The crystal itself is backed by tungsten loaded resin as shown in the figure. When sound waves are incident on the crystal the pressure variations generate voltage variations across the crystal (receiver mode). These are communicated through lead wires. In case ac power is fed through the leads the crystal oscillates and produces ultrasound waves (transmitter mode).

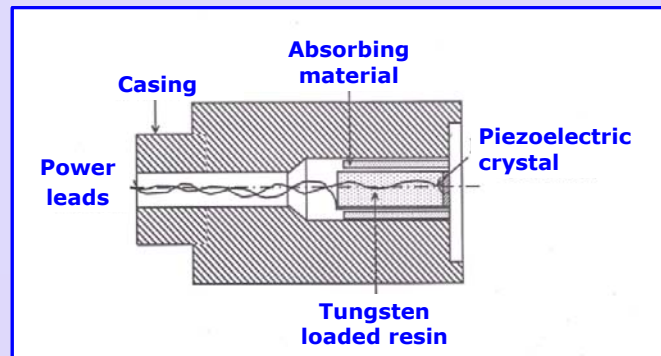


Figure 120 Piezoelectric transducer

Now we consider the arrangement shown in Figure 121. The illustration is that of measurement of velocity of a fluid in a pipe using the Doppler Effect. Two transducers are fixed on the walls as indicated. One of the transducers is a transmitter of ultrasonic waves and the second acts as a receiver for the scattered ultrasound wave. The illustration shows the transmitter and receiver to be in contact with the flow. Clamp on transducers are also possible wherein the transducers are mounted outside but in contact with the pipe wall. The latter arrangement is preferred with corrosive fluids and when it is not desirable to make holes in the pipe. In this case the ultrasound passes through the pipe wall and undergoes a change in direction that will have to be taken into account.

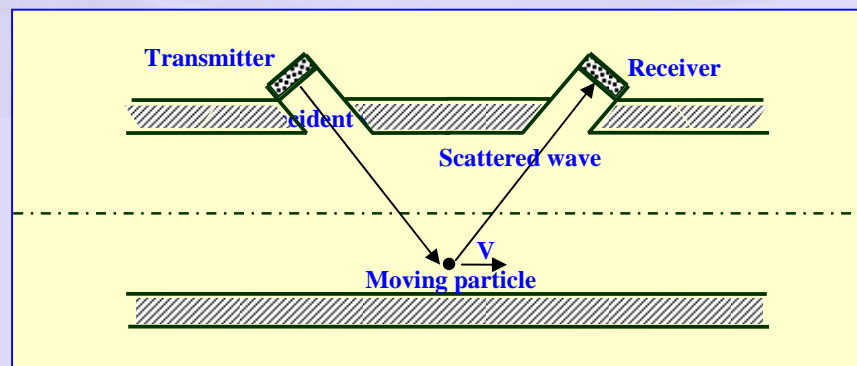


Figure 121 Measurement of fluid velocity by Doppler shift method

We assume that the particle or some naturally occurring disturbance like air bubbles in the flow, which is moving at the same speed as that of the fluid, scatters the incident wave. Figure 122 shows the schematic of the electronic circuit that is used for signal conditioning. An oscillator drives the transmitter at the desired or chosen ultrasonic frequency. Let the transmitted ultrasound wave be given by $u_t = u_{to} \cos(\omega t)$. The scattered wave then is given by $u_r = u_{ro} \cos[(\omega + \omega_D)t + \phi]$. Here u represents the signal in appropriate unit, subscripts t and r represent respectively the transmitted and received waves, ω represents the frequency of the source and ω_D is the Doppler shift and ϕ represents the phase shift. With reference to the circuit shown in Figure 105 the u 's may be taken in electrical units such as Volts or milli-volts. ω is the circular frequency that is related to the frequency as $f = \frac{\omega}{2\pi}$. If we multiply the transmitted and reflected signals together, we get

$$s = u_t u_r = u_{to} u_{ro} \cos(\omega t) \cos[(\omega + \omega_D)t + \phi] \quad (131)$$

From trigonometry, we have $\cos A \cos B = \frac{\cos(A+B) + \cos(A-B)}{2}$. Using this

identity Equation 131 may be recast as

$$s = \frac{1}{2} \left\{ \cos[(2\omega + \omega_D)t + \phi] + \cos[\omega_D t + \phi] \right\} \quad (132)$$

The signal s thus contains a high frequency component at roughly twice the input frequency (usually the Doppler shift is much smaller than the transmitted frequency) and a low frequency component at the Doppler shift frequency.

Our interest lies with the latter and hence the former is removed by extracting the latter by demodulation followed by passing the signal through a low pass filter. The Doppler shift is in the audio frequency range while the transmitted frequency is in the 100 kHz range.

In summary, the scattered radiation contains the signal at the Doppler shift frequency riding over a high frequency roughly at double the frequency of the input wave. This wave is demodulated to extract the Doppler signal that varies in the audio frequency range. A zero crossing detector, multi-vibrator and a low pass filter yields an output that is proportional to flow. Signal waveforms at various positions are also shown in the figure.

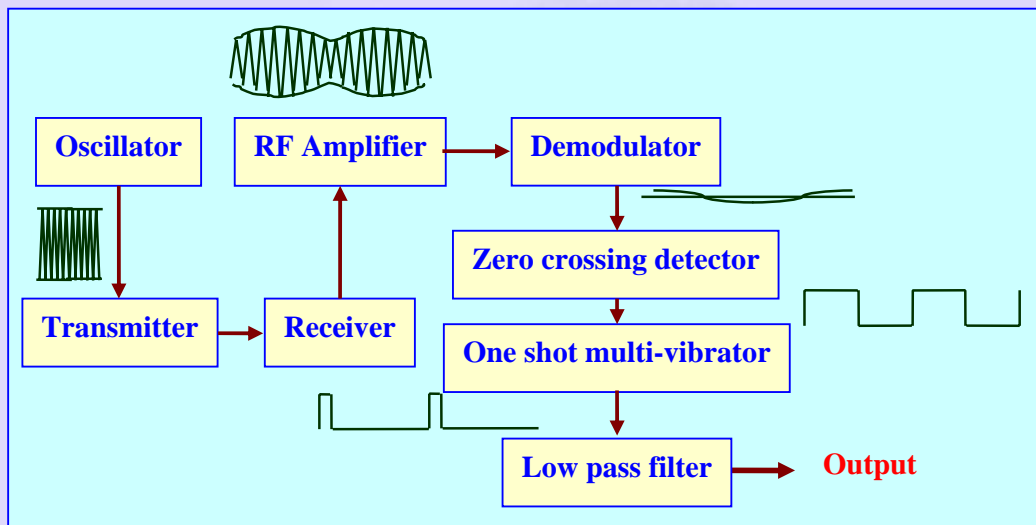


Figure 122 Circuit for measuring the Doppler shift and hence the flow

Typical performance figures for an ultrasonic Doppler flow meter are given below:

1. Over the flow range 0 to 15 m/s a repeatability of $\pm 1\%$ of full scale
2. For small pipes with well mixed slurries linearity of $\pm 1\%$ for $Re > 10^5$
3. Measurements with clamp on meters is possible up to 120°C

Consider an ultrasound system with a transmitted frequency of $f = 100$ kHz. Let the typical velocity of the fluid be $V = 1$ m/s. We shall assume that the incident and transmitted waves are almost collinear. Let the speed of the wave in the medium be $a = 350$ m/s. The wavelength of the wave is then given by

$$\lambda = \frac{a}{f} = \frac{350}{100 \times 10^3} = 0.0035 \text{ m}$$

The Doppler shift is then given by

$$f_D = \frac{V}{\lambda} = \frac{1}{0.0035} = 285.7 \text{ Hz}$$

The signal thus consists of approximately 286 Hz low frequency component riding over a wave at 200 kHz. Clearly the Doppler shifted signal is in the audible range and may in fact be heard as a 'hum' if it is connected to a speaker via an amplifier.

Laser Doppler velocity meter

In fluid mechanics research the Laser Doppler Velocimeter (LDV) is used for detailed mapping of fluid flow fields. As the name implies the radiation that is used is a highly coherent laser source. The advantage of the laser based measurement is that the beam may be focused to a very small volume thus measuring almost truly the velocity at a point. Since the focused beam is intense enough scattered energy is available to make measurements with adequate signal to noise ratio. Also high sensitivity photomultiplier tubes (PMT) are available that allow work with very small amount of scattered light. Two possible ways of operating an LDV are a) the fringe based system and b) reference beam method. We describe these two in what follows.

a) Fringe system:

Schematic of a fringe based system is shown in Figure 123. A laser source provides highly coherent light of fixed wavelength of very narrow line width. Two beams traveling parallel to each other are obtained by passing it through a partial mirror (beam splitter in figure) and then reflecting one of the beams off a mirror. These two beams are focused at a point within the flow medium as shown. A particle or some disturbance passing through the region close to the focal point will scatter energy as shown. At the focal point the two beams form an interference pattern that is in the form of a fringe system as shown as an inset in the figure. When a particle in the medium passes through this

region the scattered radiation intensity is modulated by the fringes. If the particle moves at a speed V across the fringe system, and if the fringe spacing is d , the frequency of the “burst” signal is given by $f = \frac{V}{d}$. It can be

shown that the fringe spacing is given by $d = \frac{\lambda}{2 \sin\left(\frac{\theta}{2}\right)}$ where λ is the

wavelength of the laser and θ is the angle between the two beams (see Figure 106). From these two expressions, we get

$$V = \frac{f \lambda}{2 \sin\left(\frac{\theta}{2}\right)} \quad (133)$$

The aperture helps to discard the main laser beam and collect only the scattered burst of light to be sensed by the photomultiplier tube (PMT). The burst signal has to be analyzed by suitable signal conditioning system to get the burst frequency and hence the velocity of the particle. The particle (may be smoke particles introduced in to the flow) should have very small size (and hence the mass) so that it moves with the same velocity as the fluid, without any slip.

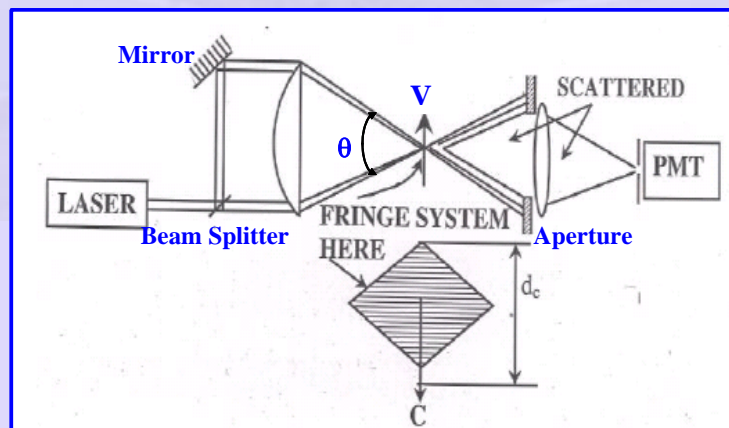


Figure 123 Fringe based laser velocity measurement

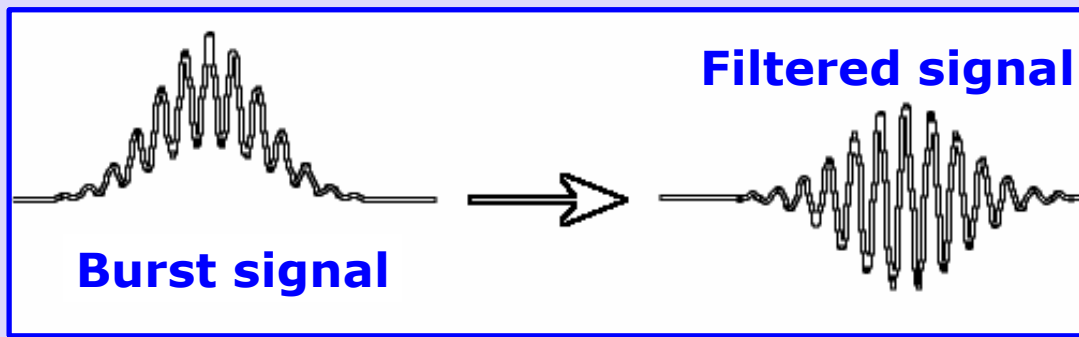


Figure 124 Scattered “burst” signal

We consider again light wave of $\lambda = 0.68 \mu m$. The speed of light in air may be taken as $c = 3 \times 10^8 m/s$. Let the two beams cross at an angle of 10° . The fringe spacing is $d = \frac{\lambda}{2 \sin\left(\frac{\theta}{2}\right)} = \frac{0.68}{2 \times \sin(5^\circ)} = 3.9 \mu m$. Note that the particle should be much smaller than the fringe spacing so that the burst signal is not ‘smeared’. Consider a scattering particle traveling with a velocity of 10 m/s. The burst signal has a frequency given by $f = \frac{V}{d} = \frac{10}{3.9 \times 10^{-6}} = 2.563 MHz$.

b) Reference beam system:

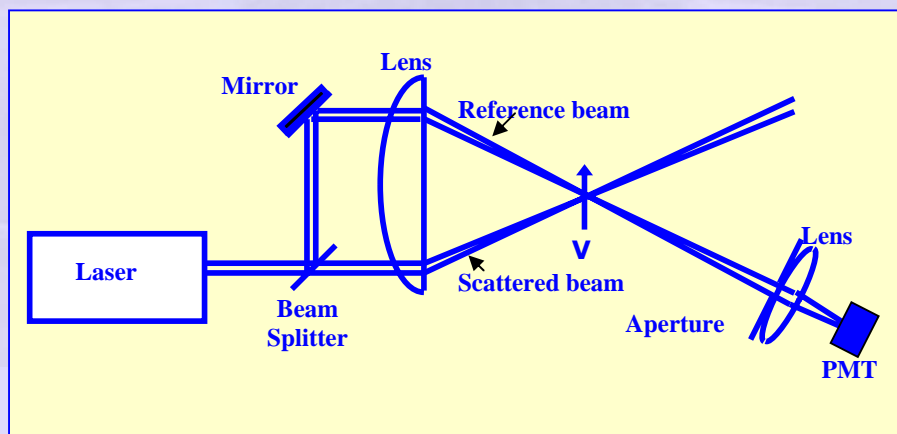


Figure 125 Schematic of the reference beam system

The schematic of the reference beam system is shown in Figure 125. Here again we cross a reference beam (weakened by a small reflectance of the mirror) and a scattered beam at the focal point of a lens with an aperture. The reference beam is directly collected by the lens and communicated to the

PMT. Radiation scattered by the scattered beam within the field of view of the lens is also communicated to the PMT. The PMT responds to the incident intensity which consists of a part that varies at the Doppler shift frequency. This rides over a dc part that is related to the mean intensity of the two beams. Again suitable electronic circuit is required to extract the Doppler shift and hence the particle velocity. Table 19 below gives the specifications of a typical laser Doppler system.



Table 19 Typical Laser Doppler systems

Specifications	Canon LV-20Z	Canon LV-50Z
Measurement Range	-200 to 2000mm/sec.	-50 to 5000mm/sec.
Focal Length	40mm	
Depth of focus	±5mm	
Laser spot size	2.4 x 0.1mm (at focal point)	
Velocity fluctuation response frequency	0 to 300Hz	
Output Signal		
Accuracy	less than ±1% of full scale	
Doppler pulse output	120 to 1000kHz	180 to 2200kHz
Measurement Certainty	<100mm/sec : ±0.2mm/sec >100mm/sec : ±0.2%	
Optical shift frequency output	200kHz, CMOS level	
Velocity display	5digit (mm/sec, m/min. selectable)	
Light source	Semiconductor laser (680nm)	

4) Time of Flight Velocimeter

Time of flight refers to the time it takes an acoustic beam to travel through a certain length in a moving medium. Since the motion of the medium affects the time of flight it is possible to use this as a means of measuring the velocity of the medium. This method does not need the presence of any scattering particles in the flow as in the case of the Doppler shift method. Consider the scheme shown in Figure 126.

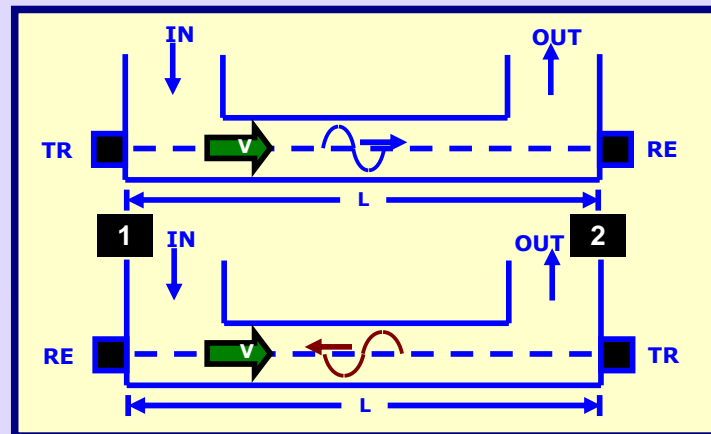


Figure 126 Schematic of the time of flight (TOF) method

An ultrasound wave pulse (of a short duration) is transmitted from 1 and travels along the fluid and reaches the receiver at 2. Along this path (referred to as the forward path) the sound wave travels at a speed of $a_f = a - V$. The

corresponding time of flight is $T_{12} = \frac{L}{a - V}$. However if the sound wave

traverses along path 2-1 (backward path) the speed of wave and the TOF are

respectively given by $a_f = a + V$ and $T_{12} = \frac{L}{a + V}$.

We then have the following:

$$T_{12} - T_{21} = \frac{L}{a - V} - \frac{L}{a + V} = \frac{2LV}{a^2 - V^2} \quad (134)$$

And also

$$T_{12} T_{21} = \frac{L^2}{a^2 - V^2} \quad (135)$$

Division of Equation 135 by Equation 134 then yields the interesting result

$$\frac{T_{12} T_{21}}{T_{12} - T_{21}} = \frac{\cancel{L^2} / (a^2 - V^2)}{2LV / \cancel{(a^2 - V^2)}} = \frac{L}{2V} \quad (136)$$

We notice that the speed of the wave has dropped off and the velocity is given by the ratio of path length and time. Thus

$$V = \frac{L}{2 \left(\frac{T_{12}T_{21}}{T_{12} - T_{21}} \right)} \quad (137)$$

Scheme shown in Figure 126 is possible when one is allowed to make a bypass arrangement so that a straight segment may be arranged as shown. This way it is possible to choose a large L so that the accurate measurement is possible. However, more often, we have the flow taking place in a pipe and the arrangement shown in Figure 127 is a feasible arrangement. In this case, as discussed earlier, it is not necessary to make any changes in the piping for making the TOF measurement.

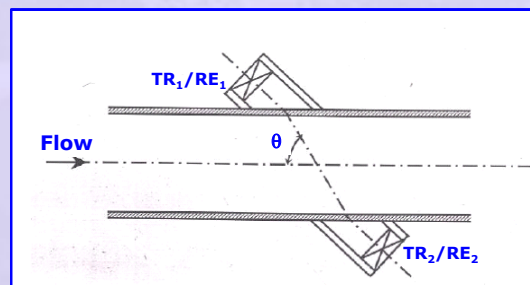


Figure 127 Clamp on type ultrasonic mean velocity meter

A variant of the above is when one is allowed to expose the ultrasound transducer to the flowing medium (transducers are said to be wetted). The schematic shown in Figure 128 also includes the schematic of the electronic circuit that is needed for making the measurement.

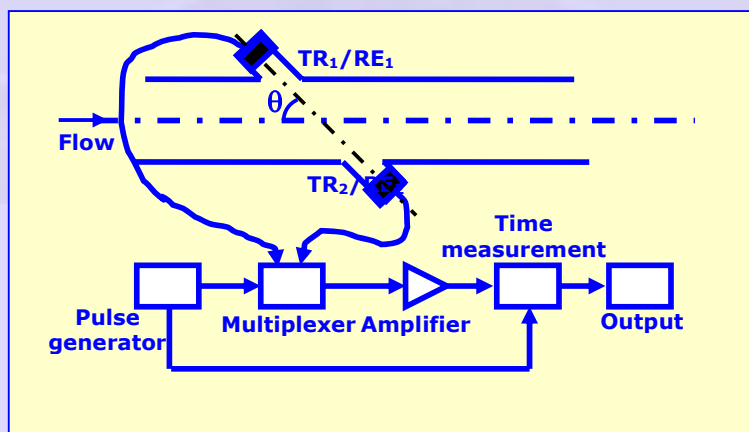


Figure 128 Ultrasonic mean velocity meter

In this case the velocity of the fluid has a component in the direction 12 and hence the equations given earlier are to be modified as under.

Let the diameter of the pipe be D . The path length is then given by $L = \frac{D}{\sin \theta}$.

Along the forward path the sound wave travels at a speed of $a_f = a - V \cos \theta$.

The corresponding time of flight is $T_{12} = \frac{D/\sin \theta}{a - V \cos \theta}$. However if the sound wave

traverses along path 2-1 (backward path) the speed of wave and the TOF are

respectively given by $a_f = a + V \cos \theta$ and $T_{21} = \frac{D/\sin \theta}{a + V \cos \theta}$.

We then have the following:

$$T_{12} - T_{21} = \Delta T = \frac{D/\sin \theta}{a - V \cos \theta} - \frac{D/\sin \theta}{a + V \cos \theta} = \frac{2DV \cot \theta}{a^2 - V^2 \cos^2 \theta} \quad (138)$$

If we assume that $V \ll a$, the second term in the denominator may be dropped to get

$$\Delta T \approx \frac{2DV \cot \theta}{a^2} \quad (139)$$

Thus the difference in times of flight is directly proportional to the velocity. If the angle θ is arranged to be 45° cotangent is 1 and the velocity is given by

$$V \approx \frac{a^2 \Delta T}{2D} \quad (140)$$

Again, we may take the ratio as earlier to get

$$\frac{T_{12} T_{21}}{T_{12} - T_{21}} = \frac{D}{2V \sin \theta \cos \theta} = \frac{D}{V \sin(2\theta)} \quad (141)$$

Again, if the angle θ is arranged to be 45° , the above reduces to

$$\frac{T_{12} T_{21}}{T_{12} - T_{21}} = \frac{D}{V} \quad (142)$$

What is interesting again is that the wave speed has dropped off. In addition the velocity of the fluid is given by the ratio of the diameter of the pipe to the

effective time that measured by the ratio. The velocity measured is the mean velocity across the path traveled by the ultrasound wave in case the fluid velocity varies across the pipe.

Consider water flowing in a pipe of 100 mm diameter at a velocity of 1 m/s. The angle θ is arranged to be 45° .

The speed of sound in water is approximately $a = 1500$ m/s. The transit times are calculated as:

$$T_{12} = \frac{D/\sin \theta}{a - V \cos \theta} = \frac{0.1/\sin 45^\circ}{1500 - 1 \times \cos 45^\circ} = 94.325 \mu s$$

$$T_{21} = \frac{D/\sin \theta}{a + V \cos \theta} = \frac{0.1/\sin 45^\circ}{1500 + 1 \times \cos 45^\circ} = 94.236 \mu s$$

Thus the time difference is only about 89 ns! Measurement of such small time differences is quite a challenge!

From Equation 142, we however, have $\frac{T_{12}T_{21}}{T_{12} - T_{21}} = \frac{D}{V} = \frac{0.1}{1} = 0.1 s!$

We see from the above that the transit times are very small and some way of increasing these are desirable. One of these is to use the arrangement shown in Figure 126. Another arrangement is to provide for multiple reflections as shown in Figure 129. The effective path is increased several fold by this arrangement.

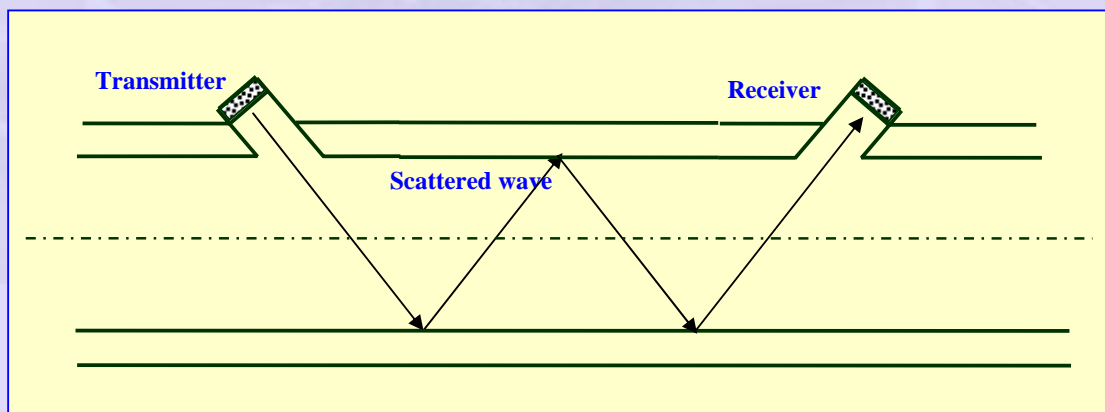


Figure 129 Method of increasing path length in TOF measurement

Simultaneous measurement of position and velocity:

We can combine TOF and Doppler shift measurements to study the velocity and the position of a scattering particle in a flowing medium. This is referred

as pulsed echo technique and is commonly used in medical blood flow measurement applications. The principle of this may be understood by referring to Figure 130.

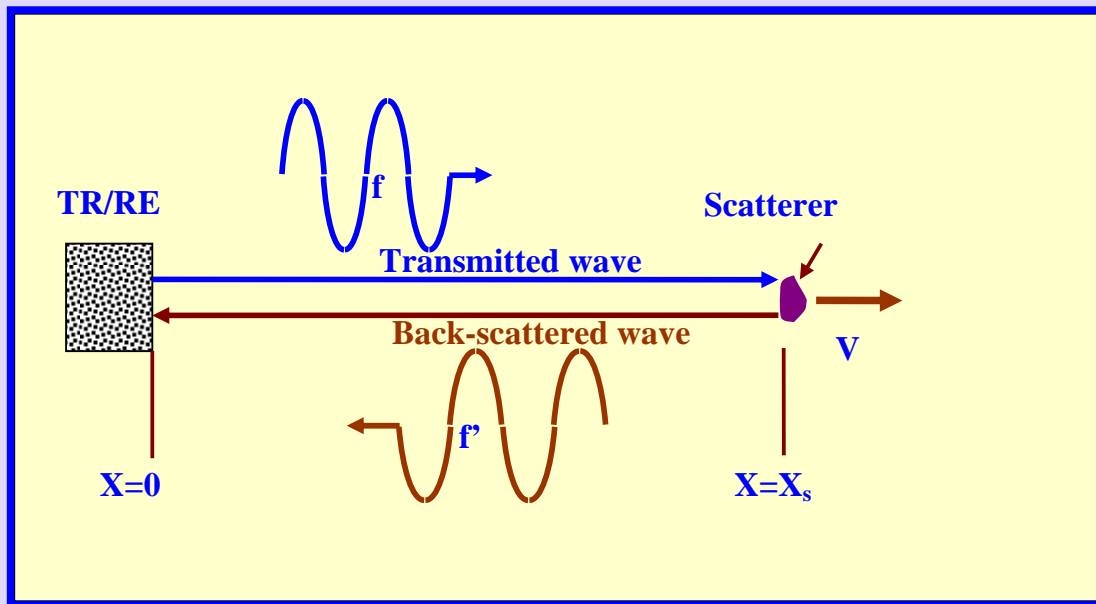


Figure 130 Simultaneous position and velocity measurement

Let us assume that a scatterer is present and is moving as shown in Figure 130. A short pulse of ultrasound is transmitted at $t = 0$ and the received pulse is analysed for both the transit time and the Doppler shift. If the velocity is small compared to a , the transit time τ is related to the position by the simple relation $\tau \approx \frac{2X_s}{a}$. At the same time if the Doppler shift is measured it is directly related to the velocity of the scatterer, as has been shown earlier. Thus both the position and velocity may be measured simultaneously. An interesting variant of this is to gate the measurement such that a reflected pulse received after a certain time only is sampled. This will correspond to a certain location of the scatterer. The corresponding Doppler shift will provide the velocity at the location specified by the gated time.

Cross correlation type velocity meter

Another method of measurement which converts velocity measurement to a time measurement is the cross correlation type of measurement. The schematic of the arrangement is shown in Figure 131. Two transmitters and receivers are arranged distance L apart as shown in the figure. A disturbance that is carried by the fluid at its own speed crosses the first transmitter-receiver pair at some time that may be taken as zero. After a certain delay the same disturbance will pass the second transmitter-receiver pair. This is schematically shown in Figure 132.

To ascertain the time accurately the product of the signal received by first receiver is multiplied by the signal from the second receiver with a variable delay time τ_d . The product will be substantially zero till the delay time is equal to the transit time. The product signal will show a non-zero blip when the delay time is the same as the transit time of the disturbance. The fluid velocity is then given by $V = \frac{L}{\tau}$. Thus the velocity measurement has been

reduced to its very definition – the ratio of path length to transit time!

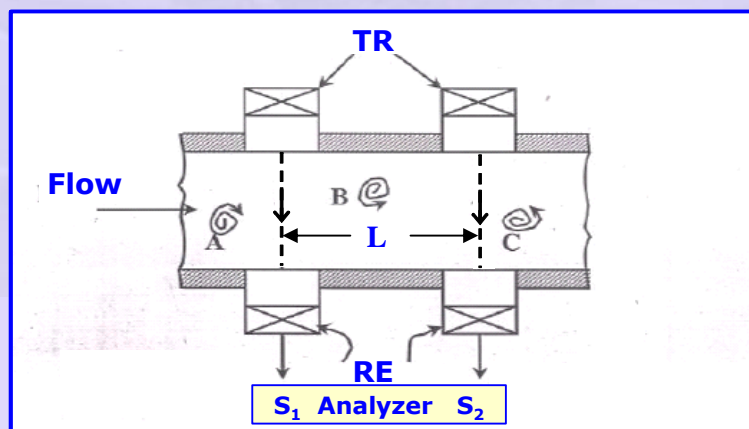


Figure 131 Cross correlation type velocity meter

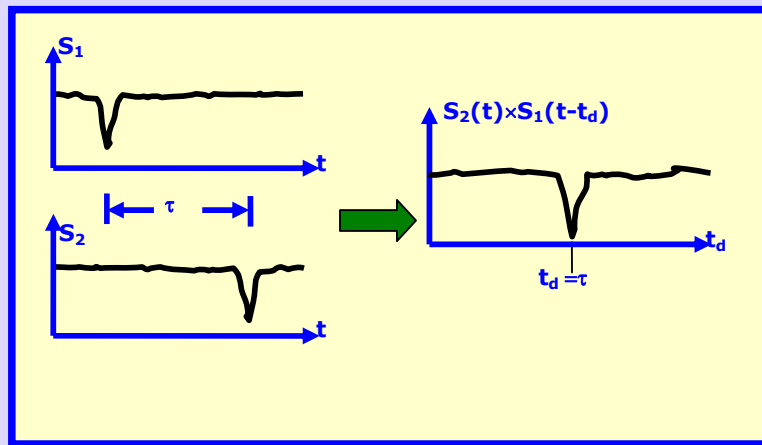


Figure 132 Cross correlation time measurement

